

Searching for $z \simeq 6$ Objects with the *HST* Advanced Camera for Surveys: Preliminary Analysis of a Deep Parallel Field

Haojing Yan, Rogier A. Windhorst and Seth H. Cohen

Department of Physics and Astronomy, Arizona State University, Tempe, AZ 85287-1504

Haojing.Yan@asu.edu, Rogier.Windhorst@asu.edu, Seth.Cohen@asu.edu

ABSTRACT

Recent results suggest that $z \simeq 6$ marks the *end* of the reionization era. A large sample of objects at $z \simeq 6$, therefore, will be of enormous importance, as it will enable us to observationally determine the exact epoch of the reionization and the sources that are responsible for it. With the *HST Advanced Camera for Surveys* (ACS) coming on line, we now have a unique opportunity to discover a significant number of objects at $z \simeq 6$. The pure parallel mode implemented for the *Wide Field Camera* (WFC) has greatly enhanced this ability. We present our preliminary analysis of a deep ACS/WFC parallel field at $|b| = 74.4^\circ$. We find 30 plausible $z \simeq 6$ candidates, all of which have $S/N > 7$ in the F850LP-band. The major source of contamination could be faint cool Galactic dwarfs, and we estimated that they would contribute at most 4 objects to our candidate list. We derived the cumulative number density of galaxies at $6.0 \leq z \leq 6.5$ as 2.3 arcmin^{-2} to a limit of 28.0 mag in the F850LP-band, which is slightly higher than our prediction. If this is not due to an underestimated contamination rate, it could possibly imply that the faint-end slope of the $z \simeq 6$ luminosity function is steeper than $\alpha = -1.6$. At the very least, our result suggests that galaxies with $L < L^*$ do exist in significant number at $z \simeq 6$, and that they could be the major sources that contributed the reionizing photons.

Subject headings: cosmology: observations — galaxies: high-redshift — galaxies: luminosity function, mass function

1. Introduction

In the last couple of years, great progress has been made in answering the grand cosmological question of when reionization of the universe began. It is now generally believed

that we have seen *the end* of the reionization at around $z = 6$. Fan et al. (2002) provided a detailed analysis of the spectra of the SDSS $z \sim 6$ quasars, and argued that the epoch of reionization could not be at a redshift much higher than 6. This is also consistent with the most recent numerical simulations of cosmological reionization (e.g., Cen & McDonald 2002), where it is suggested that the IGM is likely neutral at $z > 6.5$. On the other hand, Hu et al. (2002) reported their discovery of a $z = 6.56$ $Ly\alpha$ emitter and therefore suggested that the reionization lies beyond $z = 6.6$. Nevertheless, the detectability of $Ly\alpha$ emission line *prior* to the reionization was investigated by Haiman (2002), who pointed out that such a line, if broad enough, could still be observable, and thus the $Ly\alpha$ emitter of Hu et al. (2002) might actually lie *beyond* the epoch of the reionization. Very recently, Cen (2002) proposed a scenario that the Universe was actually reionized twice, which could also explain the seemingly-paradoxical detection of this $z = 6.56$ $Ly\alpha$ emitter.

The kinds of sources responsible for the reionization is one other question that remains open. While the strong UV spectrum of a quasar is capable of ionizing surrounding IGM out to Mpc scales, the paucity of quasars makes them unlikely the major contributors to the reionizing background. Based on the stringent constraint they obtained for the bright-end slope of quasar luminosity function at $z \sim 6$, Fan et al. (2002) pointed out that luminous quasars could not provide sufficient photons to keep the universe ionized at this redshift. However, there is still room for lower luminosity AGNs ($M_B > -23$ mag) being important reionizing sources. Alternatively, the reionizing photons could also come from star-forming galaxies, provided that a sufficient amount of Lyman continuum emission could escape from the galaxies. While the escape fraction (f_{esc}) of such emission is found to be extremely small in the local universe (Leitherer et al. 1995; Hurwitz et al. 1997), Steidel et al. (2001) derived $f_{esc} \simeq 65\%$ from the composite spectrum of a sample of 29 $z \simeq 3.4$ Lyman-break galaxies. Although such a high f_{esc} value is still under debate (see Giallongo et al. 2002), star-forming galaxies cannot be ruled out as important contributors to the reionizing background. An extreme scenario has been proposed by Ricotti (2002), who suggested that globular clusters, which can be formed outside of galaxy disks or bulges and thus have f_{esc} close to unity, were responsible for the reionization.

Obviously, we will have to first acquire a large sample of $z \simeq 6$ objects before we can settle all these issues. The *Wide Field Camera* (WFC) of the *Advanced Camera for Surveys* (ACS) on-board the HST provides an unique opportunity to discover a large number of $z \simeq 6$ objects and probe the faint end of the luminosity function (LF). To maximize its scientific return, a default pure parallel observation mode has been implemented for the WFC (Sparks et al. 2001). This mode utilizes four filters, namely F775W (SDSS-*i*), F850LP (SDSS-*z*), F475W (SDSS-*g*), and F625W (SDSS-*r*), in order of preference. Whenever there is at least one orbit of time available for parallel observation, this mode always takes images in the

F775W and F850LP bands. Given the high throughput and the wide field-of-view (FOV) of the WFC, such a strategy makes its parallel data extremely useful for selecting objects at $z \simeq 6$ by using the *drop-out* technique.

In this letter, we present our preliminary analysis of a field that is the deepest ACS/WFC parallel observation to date. We describe the data reduction in §2, followed by the $z \simeq 6$ candidate selection in §3. The comparison between the result of this study and the prediction of Yan et al. (2002) is made in §4. We conclude with a brief summary in §5. Throughout the paper, we use the AB magnitude system, and adopt a cosmological model with $(\Omega_M, \Omega_\Lambda, H_0) = (0.3, 0.7, 65)$.

2. Data and Photometry

The center of this field is $RA = 12^h43^m32^s$, $Dec = 11^\circ40'32''$ (J2000), and it is at a galactic latitude of $|b| = 74.4^\circ$. The primary observation of the visits is the WFPC2 imaging of NGC4647, which has a size of $2.9' \times 2.3'$ and the V-band total magnitude of 11.3 mag. As the border of the WFC is about $5'$ away from that of the WFPC2, the parallel field is not contaminated by the light from either this galaxy or its close neighbor, M60. The observations spanned from April 28 to June 19, 2002. Only the F775W and F850LP filters were used for the parallel imaging. In total, 15 images were taken in the F850LP-band and 27 images were taken in the F775W-band. The total exposure time in these two bands is 2.65 hours and 4.28 hours, respectively.

After combining the individual images into final stacks, we used *SExtractor* of Bertin & Arnouts (1996) to perform matched-aperture photometry by invoking its double-input mode. The F850LP stack was used for extracting sources and defining apertures, and the magnitude of each detected source was measured on the F850LP stack and the F775W stack independently, but with a same aperture. For source detection, we used a 5×5 Gaussian smoothing kernel with the FWHM of 2.0 pixels, which is approximately the same as the FWHM of a point source PSF on both stacks. The detection threshold was set to 1.8σ , and at least 4 connected pixels above this threshold were required for a source to be included. We used total magnitude (corresponding to the *mag-auto* option in SExtractor) for the photometry. The two catalogs were then merged into a master catalog, which we shall refer to as the “matched catalog”. We adopted the zeropoints used by the Great Observatories Origins Deep Survey (Dickinson & Giavalisco 2002) team for their HST Treasury program utilizing the same instrument, where they have derived the zeropoints as one electron corresponding to $m_{775W} = 25.656$ mag and $m_{850LP} = 24.916$ mag.

We assessed the F850LP-band survey limit as the following. The representative error (Δm) reported by *SExtractor* was used to calculate the S/N of each extracted source, using the simple relation of $\Delta m = 1.0857/(S/N)$. Only the sources with $S/N \geq 5$ were included in the assessment. From the source count histogram, we estimated that the survey was 100% complete to $m_{850LP} \leq 28.0$ mag. To estimate the faintest level that the F775W-band achieved, we ran *SExtractor* independently on the F775W stack with the detection threshold lowered to 1σ . We counted the number of detected objects regardless of their S/N , and found that the number count histogram reaches its peak value at 30.0 mag. Thus, for an object that is not detected in the F775W-band, it must be fainter than 30 mag in this band. We will use this result in §3.2 below.

3. Selecting $z \geq 6$ Objects

We selected $z \geq 6$ objects via the *drop-out* technique (e.g., Steidel et al. 1995) that identifies the Lyman-break signature their spectral energy distributions (SED’s). At $z \geq 4$, this signature, which is mainly due to the cosmic intervening H I absorption (Madau 1995), occurs at rest-frame wavelength of 1216 Å. At $z \simeq 6$, this signature moves out of the F775W-band and into the F850LP-band. As the area enclosed by the F850LP-band system response curve drops to half of the total value at around 9200 Å, this passband losses its efficiency at this wavelength. Therefore, the combination of these two filters is effective in identifying the Lyman-break in the redshift range of $6.0 \leq z \leq 6.5$.

3.1. Drop-out Selection

We define an object as a “F775W drop-out” if it is significantly detected in the F850LP-band but is not visible in the F775W-band. To be specific, such a source should be flagged as not detected in the F775W-band in the matched catalog, and it should have reported photometric error smaller than 0.15 mag, or equivalently, have S/N larger than 7.2, in the F850LP-band. The later constraint was rather conservative, and it was applied because at this stage we were more concerned with the reliability of the selection than its completeness at the low brightness level. At this S/N level, the survey in the F850LP-band is 100% complete to 27.5 mag.

Such criteria resulted in a candidate list of 114 objects. All these sources were then visually examined in both bands to make sure that 1) it was a real detection in the F850LP-band and 2) it was not seen in the F775W-band. This refining procedure rejected 84 objects

from the list and only 30 plausible candidates remained. We found that there were a variety of reasons that gave rise to false candidates. Besides those causes commonly seen in CCD imaging (e.g., background anomaly close to the field edges due to dithering), one other important cause is the correlated background noise that is due to the geometric correction, which accounts for about 40% of the 84 false candidates.

While it maps the off-axis ACS images back to the proper geometry, the geometric correction makes the mapped pixels non-independent. As a result, the background noise in the mapped pixels is spatially correlated, and such a correlation shows up as weak, web-like structures in the background (visible in Fig. 1). The effect of these structures is two-fold. When the object search is pushed to very faint threshold in the F850LP-band, some of these structures could be picked up as local maximum and result in false detections in this band. On the other hand, if a faint but real object is too close to such structures in the F775W-band, it could be missed by the source detection algorithm. The source detection parameters that we used to generate the matched catalog were optimized to make the detection as complete as possible while keeping the number of false objects manageable. The visual examination serves as a second safeguard procedure to keep the candidate list clean.

To independently check the reliability of these 30 candidates, we performed a simulation to test whether these objects could be recovered if they were at different places on the F850LP stack. For a given candidate, a 13×13 pixel image stamp centered on it was copied from the F850LP stack. After subtracting a constant sky background, the stamp was put at 1,000 random positions on the F850LP stack, and thus generated 1,000 artificial objects that have the same photometric properties of their prototype. *SExtractor* was then run with the same parameter setting and the number of recovered artificial objects was counted. The simulation was done for each of the 30 candidates, and we found that the median recovering rate was 88%. The recovering rate essentially remains at this level for the objects that are brighter than 28.0 mag, and drops slightly to 79% beyond this limit. Thus our candidates are deemed reliable.

Fig. 1 shows the F775W and the F850LP images of six candidates that are randomly chosen from the 30 sources. The images have been smoothed by a 5×5 boxcar to enhance the detected sources. The F850LP-band magnitude of the 30 sources ranges from 26.8 to 28.3 mag, and only three of these sources are fainter than 28.0 mag. The median magnitude of these candidates is 27.4 mag.

3.2. Possible Sources of Contamination

We visually examined the locations of these 30 candidates on each of the 15 individual F850LP-band images, and found no transient event on these locations. Therefore, any possible source of contamination must be of non-transient nature. There are three types of sources whose SED could mimic the Lyman-break signature at $z \simeq 6$, namely, strong emission-line galaxies at low redshift, elliptical galaxies, and cool dwarfs in our Galaxy. Given the sharp cut-off of the F775W-band in the red and our stringent selection criteria, we argue that none of these sources is likely to seriously contaminate our candidates:

1. *Low- z emission-line galaxies* — Such galaxies should have very strong emission lines in the F850LP-band to be included by our selection criteria. The observed equivalent width W_{obs} of such an emission line can be estimated by using $W_{obs} \simeq (\widetilde{F}_\nu / f_{\nu c}) D$, where D is the width of the F850LP passband, \widetilde{F}_ν is the average flux measured in the F850LP-band, and $f_{\nu c}$ is the continuum flux estimated from the F775W-band. Since D is about 1390 Å and a conservative lower limit of $\widetilde{F}_\nu / f_{\nu c}$ is 4, we get $W_{obs} > 5000$ Å. Considering that the system response of the F850LP-band drops to half of its peak value at around 8300 Å and 9700 Å in the blue and the red, respectively, the emission lines that are possible to produce the detected flux are $H\alpha$ (6563 Å) at $0.26 \leq z \leq 0.48$, $[OIII]$ (5007 Å) at $0.66 \leq z \leq 0.94$ and $[OII]$ (3727 Å) at $1.23 \leq z \leq 1.60$. Therefore, the smallest possible rest-frame equivalent width is still enormously high, $W = W_{obs} / (1 + 1.60) > 2200$ Å. Such emission-line galaxies should be very rare, if there is reason to believe that they exist at all. Hence, it is very unlikely that emission-line galaxies would contaminate our candidates.

2. *Elliptical galaxies* — Although the 4000 Å break in the SED of an elliptical galaxy at $1.0 \leq z \leq 1.5$ occurs in between the F775W and the F850LP bands, this break is not as steep as the Lyman-break at $z \simeq 6$. The sharp cut-off of the F775W system response in the red further helps to discriminate between these two features. Convolution of a typical SED of E/S0 galaxies (e.g., Coleman et al. 1984) at $1.0 \leq z \leq 1.5$ with the WFC system responses gives $m_{775W} - m_{850LP} \simeq 1.0$ mag, while the same synthesis for a model $z \simeq 6$ galaxy gives $m_{775W} - m_{850LP} \geq 2.0$ mag. Given that any object with $m_{775W} < 30.0$ mag should be detected in the F775W-band (see §2), all of our candidates have $m_{775W} - m_{850LP} > 1.5$ mag, among which 27 objects have $m_{775W} - m_{850LP} > 2.0$ mag. Therefore, we argue that the possible contamination rate due to elliptical galaxies is three objects at most.

3. *Cool dwarfs* — L and T type dwarfs are known to create large color discrepancy in the passbands similar to those used in this study, and it is very difficult to distinguish them without IR photometry (e.g. Fan et al. 2000). Unfortunately, we do not have any knowledge about their spatial distribution, and we have to heavily rely on very rough assumptions to estimate their contamination to our sample. Given the faintness of our candidates, it is

implausible for luminous dwarfs to enter our selection, as that would put their distances far beyond the thickness of the Galaxy. The least luminous L dwarfs currently detected have absolute magnitudes at $M_I \sim 20$ mag level (e.g. Dobbie et al. 2002). For such objects to remain undetected in the F775W-band, they would have to be at a distance of 0.6 kpc or further. Assuming an outer bound of 1.5 kpc from the Sun, the volume that our field-of-view samples is approximately 880 pc^3 . If we assume an IMF of the form $dN/dM \propto m^{-\alpha}$ with $\alpha \simeq 1$ and use the model of Haywood & Jordi (2002), the local number density of dwarfs is approximately of 0.04 pc^{-3} . Using a scale height of 0.3 kpc for the Galaxy (e.g. Liu et al. 2002), the number density extrapolated to a distance of 0.6 kpc and beyond will drop by at least a factor of ten. Thus we estimate that the contamination due to cool dwarfs is about 3–4 objects at most.

4. Comparison to Prediction

Among the 30 plausible candidates, 27 have $m_{850LP} < 28.0$ mag. The remaining three objects fall in the 28.0–28.5 mag bin where the survey begins to be severely affected by incompleteness, and, as discussed above, they are also the only three objects that could possibly be elliptical galaxies (see §3.2). These three objects are not included in the discussion below.

Taking into account that we discarded the field edges and the gap between the two CCD chips, the effective survey area is approximately 10 arcmin^2 . If we assume that cool Galactic dwarfs contribute 4 contaminants (§3.2), the number density at $6.0 \leq z \leq 6.5$ is 2.3 arcmin^{-2} . This result indicates that $L < L^*$ galaxies do exist in large number at $z \simeq 6$ as expected. We have predicted the number density of galaxies at $5.5 \leq z \leq 6.5$ in Yan et al. (2002) by extrapolating the LF measured at $z \simeq 3$ to $z \simeq 6$ and using the observational limits in the HDF-N as the normalization. The high-normalization case of our prediction gives a cumulative number density of 3.67 arcmin^{-2} to 28.0 mag. The co-moving volume at $6.0 \leq z \leq 6.5$ is about 48.7% of that at $5.5 \leq z \leq 6.5$ in our adopted model cosmology. Therefore, the number density that Yan et al. (2002) would predict for the $6.0 \leq z \leq 6.5$ range is 1.8 arcmin^{-2} . Fig. 2 shows the cumulative number density prediction adapted from Yan et al. (2002), with the result from this study added. Note that the observed number density inferred from our candidates is slightly higher than the predicted value. While the survey in the F850LP-band is complete to 28.0 mag in the matched catalog, the candidate selection is done at a much higher brightness level ($S/N \geq 7.2$) and is complete to 27.5 mag. That means the true number density at 28.0 mag could be even larger.

This discrepancy could be due to the possibility that we underestimated the contami-

nation rate of cool dwarfs. However, the higher number density could also be real. If this is the case, it implies that the actual LF is slightly different from that in Yan et al. (2002). Indeed, if we increase the normalization in Yan et al. (2002) by 50%, this higher value can be explained without violating any other existing constraints to the LF. Or alternatively, if we change the assumed faint-end slope from $\alpha = -1.6$ to -2 , this higher value can also be explained. The later possibility is of particular interest, as a steeper faint-end slope in the LF is what expected from the reionizing photon budget argument if star-forming galaxies are indeed the major sources of the reionizing photons (Silk 2002, private communication).

5. Summary

The ACS/WFC provides an unprecedented opportunity to probe the LF of $z \simeq 6$ galaxies at its faint end. The two red filters that it has, the F775W and the F850LP, are ideal for selecting such objects by identifying the Lyman-break signature at $6.0 \leq z \leq 6.5$. We present our preliminary analysis on a deep ACS/WFC parallel field. We discovered a total of 30 plausible candidates to a limit of 28.3 mag in the F850LP-band, 27 of which are to a limit of 28.0 mag. All these candidates were detected at $S/N \geq 7.2$ in the F850LP-band.

The contamination to our sample due to either emission-line galaxies or elliptical galaxies is likely negligible. The major contaminator would be cool Galactic dwarfs, whose effect is hard to quantify as their spatial distribution is not well known. To the best of our knowledge, we estimate that they could contribute at most 4 objects to the candidate list.

We derive a galaxy cumulative number density at $6.0 \leq z \leq 6.5$ as 2.3 arcmin^{-2} to a limit of 28.0 mag, which is slightly higher than our earlier prediction (Yan et al. 2002). While this higher observed value could be an illusion due to an underestimated contamination of cool Galactic dwarfs, it could also be real. If the later is the case, one possible explanation is that the faint-end slope of the actual LF at $z \simeq 6$ may be as steep as $\alpha = -2$. Given the faintness of these candidates, spectroscopic identification is extremely difficult with existing instruments. However, deep IR imaging data now feasible with the revived NICMOS will enable us to distinguish these two possibilities. At the very least, the number of plausible candidates strongly suggests that galaxies with $L < L^*$ do exist in large number at $z \simeq 6$, and that they are important contributors to the reionizing background. Future IR surveys with the JWST will allow us to map the LF beyond $z \simeq 6$ and to even fainter fluxes.

The authors would like to thank the anonymous referee for the helpful comments. We thank Dr. H. J. A. Röttgering for carefully reading the manuscript. We acknowledge funding from NASA/JWST Grant NAG5-12460.

REFERENCES

- Bertin, E. & Arnouts, S. 1996, A&AS, 117, 393
- Cen, R. 2002, astro-ph/0210473, submitted to AJ
- Cen, R. & McDonald, P. 2002, ApJ, 570, 457
- Coleman, G., Wu, C.-C. & Weedman, D. 1980, ApJS, 43, 393
- Dobbie, P. D., et al. 2002, MNRAS, 331, 445
- Dickinson, M. & Giavalisco, M. 2002, astro-ph/0204213
- Fan, X., et al. 2000, AJ, 119, 928
- Fan, X., et al. 2002, AJ, 123, 1247
- Giallongo, E., et al. 2002, ApJ, 568, L9
- Haiman, Z. 2002, ApJ, 576, L1
- Haywood, M. & Jordi, C. 2002, in EAS Pub. Ser. 2, GAIA: A European Space Project, ed. O. Bienayme & C. Turon, 199.
- Hu, E. M., et al. 2002, ApJ, 576, L99
- Hurwitz, M., Jelinsky, P., & Dixon, W. 1997, ApJ, 481, L31
- Leitherer, C., et al. 1995, ApJ, 454, L19
- Liu, M. C., et al. 2002, ApJ, 568, L107
- Madau, P. 1995, ApJ, 441, 18
- Ricotti, M. 2002, MNRAS, 336, L33
- Sparks, W. B., et al. 2001, ACS Default (Archival) Pure Parallel Program (ISR01-06)
- Steidel, C. C., Pettini, M., & Hamilton, D. 1995 AJ, 110, 2519
- Steidel, C. C., Pettini, M., & Adelberger, K. L. 2001 ApJ, 546, 665
- Yan, H., et al. 2002, ApJ, 580, 725

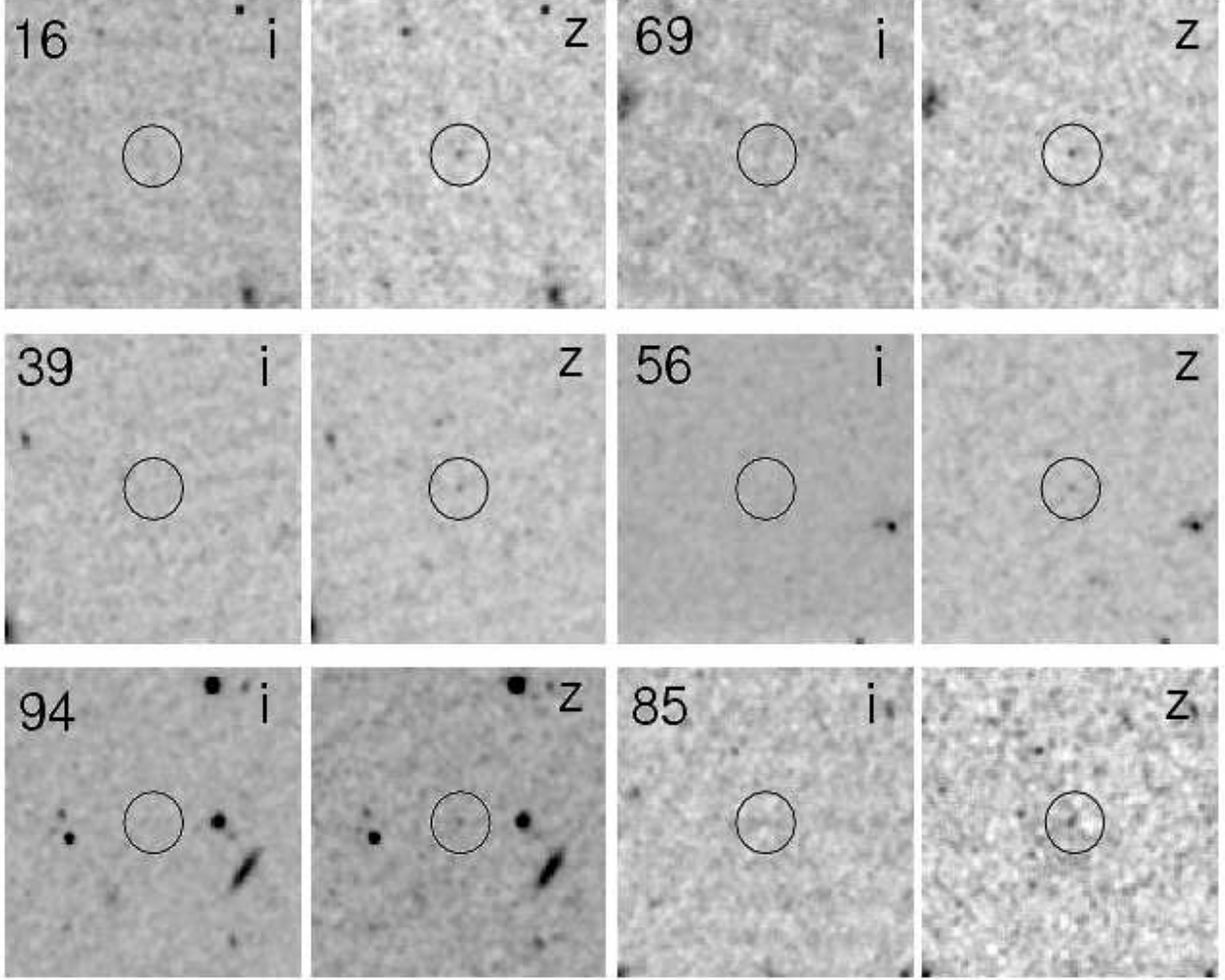


Fig. 1.— The image stamps in the F775W (labeled as *i*) and F850LP (labeled as *z*) bands for six objects that are randomly chosen from our candidate list. The images are $7''$ on a side, and have been smoothed by a 5×5 boxcar. The ID's of these candidates are label to the left of the F775W-band images, and the small circles indicate the locations of the candidates. All the 30 candidates have $S/N \geq 7.2$ in the F850LP band, and their median magnitude in this band is 27.4 mag.

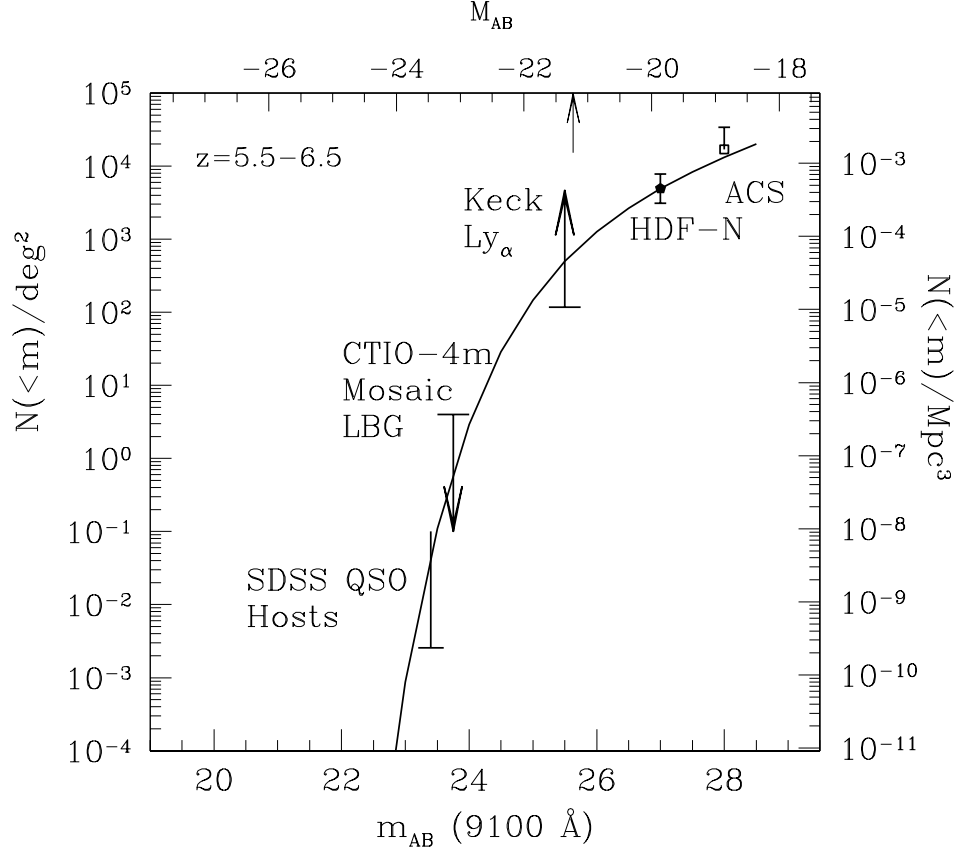


Fig. 2.— The cumulative number density of galaxies at $5.5 \leq z \leq 6.5$ inferred from the number of $6.0 \leq z \leq 6.5$ candidates found in this deep ACS parallel field is slightly higher than our prediction in Yan et al. (2002, Figure 1), which was obtained by extrapolating the LF at $z \simeq 3$ to 6 and using the few available data in the HDF-N as the normalization. For clarity, only the prediction of the high-normalization case for a $(\Omega_M, \Omega_\Lambda) = (0.3, 0.7)$ universe is reproduced here (the solid line). The M^* value is marked by an arrow on the absolute magnitude scale on the top. This prediction is consistent with nearly all the known constraints at the flux limit of brighter than 27.0 mag (see Yan et al. 2002 for details). Our current result (the open square) puts a new constraint at 28.0 mag. The one-sided error indicates the upper limit that can be inferred from our result by assuming our candidate search suffers a 50% incompleteness at the 27.5–28.0 magnitude bin (see text). If the high observed value is real, it could suggest that the faint-end slope of the LF is steeper than $\alpha = -1.6$.